

## CONTENTS C through D

---

Hydration State of Lherzolithic Shergottite ALH 77005: Evidence from Rehomogenized Melt Inclusions <i>C. Calvin and M. Rutherford</i> .....	5096
Intracrystalline Transformation of Olivine to Ringwoodite in the Sixiangkou Meteorite <i>M. Chen, H. Li, A. El Goresy, J. Liu, and X. Xie</i> .....	5006
Post Stishovite in Shergottites NWA 856 and Zagami: A Cathodoluminescence Study <i>H. Chennaoui Aoudjehane and A. Jambon</i> .....	5214
A Cathodoluminescence Study of Cristobalite and K-Feldspar in the Nakhlite MIL03346 <i>H. Chennaoui Aoudjehane, A. Jambon, and O. Boudouma</i> .....	5220
Kinetics of Phyllosilicate Formation in Hydrated Magnesiosilicate Smokes <i>L. J. Chizmadia and J. A. Nuth III</i> .....	5166
Experiments on Oxygen Isotope Exchanges Between Silicate-Melt and O <sub>2</sub> Gas During Brief Melting Using CO <sub>2</sub> Laser and Their Implications to Oxygen Isotopic Heterogeneity <i>B.-G. Choi and M. Kusakabe</i> .....	5158
Transport in the Solar Nebula: Implications for the Depletion of Moderately Volatile Elements in Chondritic Meteorites <i>F. J. Ciesla</i> .....	5151
Multivariate Analysis of In Situ and Ex Situ Martian Impact Glass <i>B. A. Cohen</i> .....	5272
The Effects of Permeability-driven Water Transport on the Evolution of CM Parent Bodies <i>R. F. Coker, B. A. Cohen, and P. A. Bland</i> .....	5278
Rubble Piles or Planets? Implications for Meteorite Parent Bodies <i>G. J. Consolmagno and D. T. Britt</i> .....	5113
Mass-dependent Fractionation of Nickel Isotopes in IIIAB Iron Meteorites <i>D. L. Cook, M. Wadhwa, R. N. Clayton, P. E. Janney, N. Dauphas, and A. M. Davis</i> .....	5167
Mg Isotopes Fractionation in Melilite in an Allende Type-A Inclusion: A High-Precision, High-Spatial Resolution Approach <i>M. Cosarinsky, K. D. McKeegan, I. D. Hutcheon, and S. Fallon</i> .....	5309
Thermal Processes of the 4 Kyr BP Oceanic Impact Based on Carbon and Mineral Phase Association in Melt Products <i>M.-A. Courty, B. Deniaux, A. Crisci, K. Grice, P. Greenwood, M. Mermoux, D. Smith, and M. Thiemens</i> .....	5157
A Search for Extraterrestrial Chromite Across the Cretaceous-Paleogene Boundary at Gubbio, Italy <i>A. Cronholm and B. Schmitz</i> .....	5058
First Systematic TEM/NanoSIMS Coordinated Study of Crystal Structure and Isotopic Composition of Presolar Silicon Carbide <i>T. L. Daulton, F. J. Stadermann, T. J. Bernatowicz, S. Amari, and R. S. Lewis</i> .....	5260

Theory of Isotopic Fractionation During Phase Growth in a Diffusion-limited Regime <i>N. Dauphas</i> .....	5162
Quantitative Mapping of Melilite Elemental Composition in Refractory Inclusions <i>A. M. Davis</i> .....	5354
Thermal Annealing of Amorphous Silicates: The Behaviour of Silicate Dust in Protoplanetary Discs <i>C. Davoisne, Z. Djouadi, H. Leroux, L. d'Hendecourt, A. P. Jones, and D. Deboffle</i> .....	5182
Can the Water Pressure in the Accretion Disk Sustain Water Adsorption on Olivine? <i>N. H. de Leeuw, M. Stimpfl, C. R. A. Catlow, M. J. Drake, P. A. Deymier, and A. W. Walker</i> .....	5015
Manganese-rich Phases in CM Chondrites: Mn-Cr Systematics of Carbonates and Silicates <i>S. de Leuw, A. E. Rubin, and J. T. Wasson</i> .....	5168
Calculations of Heating Caused by Impacts of Porous Bodies in Then Early Solar System <i>P. S. DeCarli and J. T. Wasson</i> .....	5163
Induction Heating in Asteroids Part 1: Observations and Theory <i>D. N. Della-Giustina, C. A. Marsh, J. Giacalone, and D. S. Lauretta</i> .....	5380
Identification of a Common R-Chondrite Impactor on the Ureilite Parent Body <i>H. Downes and D. W. Mittlefehldt</i> .....	5147
Origin of the Halogens in the Dark Matrix of Rumuruti <i>G. Dreibus, W. Huisl, B. Spettel, and R. Haubold</i> .....	5060
Is Martian Surface Type 1 Mildly Alkaline?: Results from New Linear Deconvolutions of Surface Types 1 and 2 <i>T. L. Dunn and H. Y. McSween Jr.</i> .....	5008
The Micrometeorite Mass Flux as Recorded in Dome C Central Antarctic Surface Snow <i>J. Duprat, C. Engrand, M. Maurette, F. Naulin, G. Kurat, and M. Gounelle</i> .....	5239

**HYDRATION STATE OF LHERZOLITIC SHERGOTTITE ALH 77005: EVIDENCE FROM REHOMOGENIZED MELT INCLUSIONS.**

C. Calvin<sup>1</sup> and M. Rutherford<sup>1</sup>. <sup>1</sup>Brown University. E-mail: Christina\_Calvin@Brown.edu.

**Introduction:** Several lines of evidence suggest that water was once abundant on the surface of Mars. There are broad implications to the discovery of water that include the search for martian life and the evolution of the martian surface. However, the source of surficial martian water is less clear. [1] discusses models where surficial martian water originated from impacts. However, studies of martian meteorites suggest that some of the surficial water may have originated within the martian mantle [2, 3, 4]. This study examined rehomogenized, olivine-hosted melt inclusions in lherzolitic shergottite ALH 77005 [5] to assess the hydration state of the parental melt. Because rehomogenization of these samples was performed using a graphite buffer, H<sub>2</sub>O would have partitioned into the CO phase generated during the experiment. Therefore, we have used other lines of evidence to discuss the hydration state of ALH 77005.

**The Partitioning of Chlorine into a Vapor Phase:** Chlorine strongly partitions into a water rich vapor or fluid phase [6, 7]. We examined the chlorine content of our rehomogenized melt inclusions and found that chlorine increases by two orders of magnitude from the early crystallizing olivine (100 ppm) to the later crystallizing low-Ca pyroxene (10,000 ppm). This indicates several things. 1) If there was H<sub>2</sub>O in the melt inclusions chlorine should have partitioned into the vapor phase generated during the experiment. As the chlorine contents of the melt inclusions remain high, it is unlikely there was any water-bearing vapor generated during the experiment. 2) The increase in chlorine has two likely origins. Chlorine could have increased during crystallization of the rock. However, P<sub>2</sub>O<sub>5</sub> was high in the melt and therefore chlorine may have behaved compatibly during crystallization of phosphate phases. The other alternative is that chlorine was added through addition of new magma or through a metasomatising agent.

**The Role of Water in Plagioclase Crystallization:** Plagioclase crystallization is particularly sensitive to the water content of the magma. At low water contents, the crystallization of plagioclase occurs at lower Al<sub>2</sub>O<sub>3</sub> content. This is because H<sub>2</sub>O depolymerizes the melt, inhibiting plagioclase nucleation. In crystallization experiments on the parental melt composition of Chassigny, [8] showed that plagioclase crystallization in a hydrous-magma occurred at higher Al<sub>2</sub>O<sub>3</sub> and that the onset of plagioclase crystallization was delayed, changing the crystallization sequence of the rock. Through our rehomogenization experiments, we determined that plagioclase crystallization occurred at ~3 wt % MgO. Crystallization experiments are in progress to determine the implications of this Al<sub>2</sub>O<sub>3</sub> concentration for a hydrous parental magma.

**References:** [1] Owen, T. (1992) in *Mars* 818-834 pp. [2] Dann, J.C. et al. (2001) *Geochimica et Cosmochimica Acta* 36: 793-806. [3] Watson, L.L. et al. (1994) *Science* 265: 86-90. [4] Lentz et al. (2001) 65: 4551-5465. [5] Calvin, C. and Rutherford, M.J. (2005) Abstract #1697. 37<sup>th</sup> Lunar & Planetary Science Conference. [6] Mathez, E. A. and Webster, J. D. 2005. *Geochimica et Cosmochimica Acta* 69: 1275-1286. [7] Metrich, N. et al. 2001. *Journal of Petrology* 42: 1471-1490. [8] Minitti, M.E. and Rutherford, M.J. 2000. *Geochimica et Cosmochimica Acta* 64: 2535-2547.

### INTRACRYSTALLINE TRANSFORMATION OF OLIVINE TO RINGWOODITE IN THE SIXIANGKOU METEORITE.

M. Chen<sup>1</sup>, H. Li<sup>2</sup>, A. El Goresy<sup>3</sup>, J. Liu<sup>2</sup>, X. Xie<sup>1</sup>. <sup>1</sup>Guangzhou Institute of Geochemistry, CAS, 510640 Guangzhou, China. mchen@gig.ac.cn. <sup>2</sup>Institute of High Energy Physics, CAS, 100039 Beijing, China. <sup>3</sup>Bayerisches Geoinstitut, Universität Bayreuth, D-95440 Bayreuth, Germany.

**Introduction :** The transformation of olivine to ringwoodite can proceed by incoherent intercrystalline diffusion-controlled [1] or interface-controlled [2] mechanism, as well as coherent intracrystalline martensitic transformation [3] or a nucleation and growth mechanism [4]. Natural ringwoodite found in shocked meteorites occurs mainly as fine-grained polycrystalline aggregates formed through a phase transition of olivine [5]. Recently, we found natural occurrence of lamellar ringwoodite in olivine of the Sixiangkou L6 chondrite.

**Meteorite:** Sixiangkou meteorite contains a number of shock veins up to several millimeters in thickness. The veins contain abundant high-pressure minerals including ringwoodite, majorite, majorite-pyropite garnet and magnesio-wüstite, for which the shock-produced pressure and temperature of about 20 GPa and 2000°C were inferred.

**Results and discussion:** In addition to polycrystalline aggregate of ringwoodite inside the shock veins, we found the lamellar ringwoodite in olivine within and neighboring the shock veins. Three kinds of lamellar ringwoodite were identified in some olivine grains by Raman spectroscopy: (a) the lamellae occurring in the {101} planes of olivine inside the shock veins. (b) the lamellae occurring in the (100) plane of olivine outside the shock veins. (c) the lamellae occurring in planar and irregular fractures of olivine outside the shock veins. Widths of ringwoodite lamellae are mostly from 0.1 to 2  $\mu\text{m}$ . FeO-content of lamellae is a few percent higher (22.51 wt.%) than that of olivine matrix (21.86 wt.%).

The compositional difference between the lamellae and olivine matrix indicating that the Mg-Fe interdiffusion should have taken place between olivine and crystallizing ringwoodite at high pressures and high temperatures. Formation of these lamellae shows a diffusion-controlled nucleation and growth of ringwoodite along deformation-produced planar defects including stacking faults and fractures in olivine. It appears that lamellar ringwoodite have incoherently nucleated and grew along all kinds of planar defects in olivine.

Our results indicate that the P-T condition available for an intracrystalline olivine-ringwoodite transformation during the shock metamorphism of this meteorite might last from seconds to minutes, a time much longer than previously assumed duration of high pressure and temperature locally prevailed in the shocked meteorite, especially along the shock veins. These new data should bring new insight into mechanisms of olivine-ringwoodite phase transitions in the lower mantle and subducting lithosphere.

**References:** [1] Sung C. M. and Burns R. G. 1976. *Earth Planet. Sci. Lett.* 32: 165-170. [2] Mosenfelder J. L. et al. 2001. *Phys. Earth Planet. Inter.* 127: 165-180. [3] Poirier J. P. 1981. *Phys. Earth Planet. Inter.* 26: 179-187. [4] Kerschhofer L. et al. 1996. *Science* 274, 79-81. [5] Price G. D. et al. 1979. *Contrib. Mineral. Petrol.* 71, 211-218. [6] The author gratefully acknowledges the support of K. C. Wong Education Foundation, Hong Kong.

**POST STISHOVITE IN SHERGOTTITES NWA 856 AND ZAGAMI: A CATHODOLUMINESCENCE STUDY.** H. Chennaoui Aoudjehane<sup>1,2</sup>, A. Jambon<sup>2</sup>, <sup>1</sup>Université Hassan II Ain Chock, Faculté des Sciences, Equipe Géoressources, BP 5366 Maârif Casablanca Morocco (e-mail: [chennaoui\\_h@yahoo.fr](mailto:chennaoui_h@yahoo.fr)), <sup>2</sup>Université Pierre et Marie Curie-Paris6 Laboratoire MAGIE, Case 110, 4 place Jussieu, 75252 Paris France (e-mail: [jambon@ccr.jussieu.fr](mailto:jambon@ccr.jussieu.fr))

The physical state of silica is a very useful index of shock in meteorites. Its study has been revived by the discovery of high pressure silica in Shergotty of the  $\alpha\text{PbO}_2$  and  $\text{ZrO}_2$  structure [1-4]. Shergottites usually contain a few percent of silica with varied textures depending on their location in the rock.

Cathodoluminescence (CL) imaging and spectroscopy is a powerful technique which enables easy identification of tridymite, cristobalite, quartz, coesite, stishovite and high/low pressure silica glass [5]. This was cross checked previously by Raman spectroscopy on reference samples and shergottites [5]. According to its textural signature we suspected the presence of post stishovite as described previously [1, 2], but we were unable to collect unambiguous CL spectra with the additional difficulty that Raman spectroscopy is destructive to this phase.

The strong luminescence of stishovite enables easy collection of its CL spectra. In addition, imaging at the maximum wavelength of stishovite permits to locate this phase rapidly and efficiently even when small grains are present and throughout a polished section. The luminescence of high pressure silica glass is weaker but the large number of areas with pure HP silica glass and their significant size permitted to record its spectrum without difficulty.

The problem with post stishovite is of another kind. The only way to recognize post stishovite was from its textural aspect; Raman spectroscopy must be avoided and all grains for which electron or X-ray diffraction patterns had been obtained were all extracted previously from the sections. After a systematic survey of the putative grains we could distinguish between stishovite, HP glass and spectra differing from all the silica phases studied so far. Such CL spectra are weaker than those of either HP glass or stishovite. It also appears that post stishovite does never occur alone, but always mixed with HP glass or Stishovite blurring its specific luminescence. Using this procedure, we could detect the presence of post stishovite in two shergottites NWA 856 and Zagami where it was not recognized previously [6].

CL appears an easy and powerful technique for identifying silica and particularly post stishovite in shocked meteorites. Unlike Raman spectroscopy it remains harmless to the samples. It is far more practicable than X-ray or electron diffraction patterns. The presence of post stishovite in all shergottites investigated so far is a strong argument to suggest a shock intensity of at least 40 GPa.

**References:** [1] Sharp T.G. et al. 1999. *Science* 284, 1511-1513. [2] El Goresy A. et al. 2000. *Science* 288, 632-634. [3] Malavergne V. et al. 2001, *MAPS* 36, 1297-1305. [4] El Goresy A. et al. 2004. *Jour. Phys. Chem. Sol.* 65, 1597-1608. [5] Chennaoui Aoudjehane H. et al. 2005. *MAPS* 40, 967-979. [6] Chennaoui Aoudjehane H. et al. 2006. Abstract #1036. 37th Lunar and Planetary Science Conference.

**A CATHODOLUMINESCENCE STUDY OF CRISTOBALITE AND K-FELDSPAR IN THE NAKHLITE MIL03346.** H. Chennaoui Aoudjehane<sup>1,2</sup>, A. Jambon<sup>2</sup> and O. Boudouma<sup>3</sup>, <sup>1</sup>Université Hassan II Ain Chock, Faculté des Sciences, Equipe Géoresources, BP 5366 Maârif Casablanca Morocco (e-mail : [chennaoui\\_h@yahoo.fr](mailto:chennaoui_h@yahoo.fr)), <sup>2</sup>Université Pierre et Marie Curie-Paris6 Laboratoire MAGIE, Case 110, 4 place Jussieu, 75252 Paris, France (e-mail: [jambon@ccr.jussieu.fr](mailto:jambon@ccr.jussieu.fr)), <sup>3</sup>Université Pierre et Marie Curie-Paris6 Service de microscopie électronique à balayage, Case 110, 4 place Jussieu 75252 Paris, France (e-mail: [boudouma@ccr.jussieu.fr](mailto:boudouma@ccr.jussieu.fr)).

Shock intensity in Martian meteorites has been actively studied in recent years to understand their formation and ejection from their parent body. The analysis of high-pressure phases like stishovite, post-stishovite, majorite, hollandite or maskelynite in shergottites permits to constrain the intensity of the shock between 30 and 90 GPa [1- 4]. Nakhrites are definitely less shocked and none of them contain high-pressure minerals.

Cathodoluminescence (CL) spectroscopy is an easy approach for determining which polymorphs of silica or other silicates are present in thin or polished sections of meteorites [5]. We applied this technique to the determination of silica and feldspar speciation in the nakhrite MIL03346. Notice that a previous CL study of MIL03346, with a comparison to Lafayette, was restricted to imaging [6].

CL images and spectra have been recorded by the cathodoluminescence system in the scanning electron microscope (SEM) of the UPMC (Université Pierre et Marie Curie Paris VI) a detailed description of which can be found in [5]. Backscattered electron (BSE) images of the mesostasis have been collected first. Mineralogy and texture are in agreement with previous results obtained on different sections [7- 10]. Details of the images show subhedral grains of silica, euhedral grains of pyroxene and dendritic oxides. The strong luminescence of the K-FP irradiates the whole mesostasis, of CL images, hiding the weaker luminescence of silica. CL Spectra restricted to much smaller areas permit to identify cristobalite [11].

The shock intensity in MIL03346 is low in agreement with that of other nakhrites, much weaker in comparison to shergottites [11]. The presence of cristobalite confirms that it is undoubtedly less than 0.1 GPa. Statistical considerations on the number of nakhrites compared to shergottites suggest that either, their number is unreasonably above the statistical expectation or more likely that the shock recorded in shergottites is not related to their ejection from their parent body.

**References:** [1] Stöffler D. 2000. abstract #1170, 31th LPSC. [2] Malavergne V. et al. 2001. MAPS **36**, 1297-1305. [3] El Goresy A. et al. 2000. Science **288**, 632-634. [4] Beck P. et al. 2005. abstract #1333 36th LPSC. [5] Chennaoui Aoudjehane H. et al. 2005. MAPS **40**, 967-979. [6] Rost D. and Vincenzi E.P 2005. MAPS **40**, A130. [7] McKay G.A. and Schwandt C. 2005. abstract #2351, 36th LPSC. [8] Rutherford M.J. et al. 2005. abstract #2233 36th LPSC. [9] Stopar J.D. et al. 2005. abstract #1547 36th LPSC. [10] Sautter V. et al 2005. MAPS **40**, A134. [11] Chennaoui Aoudjehane H. et al. 2006. abstract 1037 37<sup>th</sup> LPSC.

### KINETICS OF PHYLLOSILICATE FORMATION IN HYDRATED MAGNESIOSILICATE SMOKES.

L. J. Chizmadia<sup>1,2</sup> and J. A. Nuth III<sup>3</sup>. <sup>1</sup>Institute for Astronomy, University of Hawai'i, Honolulu, HI 96822 E-mail: lchiz@ifa.hawaii.edu. <sup>2</sup>Hawai'i Institute for Geophysics and Planetology, Honolulu, HI 96822. <sup>3</sup>Astrochemistry Laboratory, NASA Goddard Space Flight Center, Greenbelt, MD 20771.

**Introduction:** Amorphous non-stoichiometric silicate smokes produced by combustion from gas-phase precursors have similar infrared spectra as the materials observed in circumstellar and cometary dust [1]. In addition, amorphous silicate materials have been reported in the matrices of several primitive carbonaceous chondrites [e.g. 2-4]. TEM characterization of these smokes revealed chains of rounded amorphous particles 10-50 nm in size [5-6]. In a continued effort to explore the possibility that the matrices of chondritic meteorites could have contained an amorphous, non-stoichiometric component similar to the smokes, we have set up a series of hydration experiments at temperatures consistent with the oxygen isotope studies of CM2 chondrites [e.g. 7]: room temperature (~22°C) and refrigerated at 5°C.

**Results:** The Mg-smokes react immediately with H<sub>2</sub>O to form a hydrated amorphous gel [8]. After 2 days, TEM characterization of samples at both temperatures show incipient nanocrystals [8]. These results are consistent with hydration experiments performed at 84 °C and 150 °C [9]. We have tracked the rate of growth of the incipient crystals during hydration experiments at 5°C and 22°C. The phyllosilicates are first detectable at 2 days and show elongated shapes with lattice fringes, which are highly sensitive to the electron beam. The first observed crystals have an average length of 92±33 and 103±66 nm (at 5°C and 22°C, respectively) and their growth is linear until 56 days (260±57 and 218±54 nm at 5°C and 22°C, respectively). At 73 days, the 5°C samples exhibit large blocky crystals that are an order of magnitude larger than the elongated phyllosilicates in the previous time step. Interestingly, the phyllosilicates in the samples run at 22°C continue their linear growth to an average size of 328±123 nm at 112 days, with no sign of the larger blocky crystals seen in the 5°C samples.

**Discussion:** The similarity in crystal sizes between the batches run at 5°C and 22°C does not offer a way to distinguish between the two temperatures; the phyllosilicates from both temperatures are similar to those observed in primitive chondrites. However, the blocky crystals observed in the samples hydrated at 5°C for ≥73 days have not been reported. This may indicate that the alteration of chondritic matrices occurred at higher temperatures and/or for a shorter time period. One caveat is that these experiments involved an excess of water compared to silicate and this extra room may have allowed the formation of the large blocks observed. More experiments are needed where more confined matrices are explored.

**References:** [1] Nuth J. A. et al. 2002 *Meteoritics & Planetary Science* 37 1579-1590. [2] Barber D. J. 1981 *Geochimica et Cosmochimica Acta* 45 945-970. [3] Brearley A. J. 1993 *Geochimica et Cosmochimica Acta* 57 1521-1550. [4] Greshake A. 1998 *Geochimica et Cosmochimica Acta* 61 437-452 [5] Rietmeijer F. J. M. et al. 1986 *Icarus* 66 211-222. [6] Fabian D. et al. 2000 *Astronomy & Astrophysics* 364 282-292. [7] Clayton R. N. & Mayeda T. K. 1984 *Earth & Planetary Science Letters* 67 151-161. [8] Chizmadia L. J. et al. 2006 Abstract #2187. 37<sup>th</sup> Lunar & Planetary Science Conference. [9] Rietmeijer F. J. M. et al. 2004 *Meteoritics & Planetary Science* 39 723-746.

**EXPERIMENTS ON OXYGEN ISOTOPE EXCHANGES BETWEEN SILICATE-MELT AND O<sub>2</sub> GAS DURING BRIEF MELTING USING CO<sub>2</sub> LASER AND THEIR IMPLICATIONS TO OXYGEN ISOTOPIC HETEROGENEITY.**

B.-G. Choi<sup>1</sup> and M. Kusakabe<sup>2</sup>. <sup>1</sup>Dept. of Earth Science Education, Seoul Nat'l University. bchoi@snu.ac.kr. <sup>2</sup>ISEI, Okayama University.

**Introduction:** Oxygen isotopic heterogeneity preserved especially in primitive meteorites is interpreted as results of mixing between two or more oxygen reservoirs that had existed prior to or during the formation of chondritic materials [1]. Many models have been proposed for the nature of the reservoirs, including recent models of CO self shielding [2-4]. However, there are few experimental and theoretical studies for O isotope exchanges between oxygen-bearing phases in the nebula [e.g., 5]. Here we report preliminary results on O isotope exchange reactions between silicate melts and O<sub>2</sub> gas during brief heating using an on-line CO<sub>2</sub> laser-BrF<sub>5</sub> fluorination system [6].

**Experiments:** Olivine grains of Eagle station pallasite, bulk samples of Allende (CV3), Kainsaz (CO3), Duwun (L6) were used as starting materials. About 1-4 mg of these samples were placed in Ni holder and briefly (30 sec to 10 min) heated with defocused CO<sub>2</sub> laser while the chamber was filled with small amount of O<sub>2</sub> gas (OKAO;  $\delta^{18}\text{O} = 17.5\text{‰}$  and  $\Delta^{17}\text{O} = -0.3\text{‰}$ ), where  $P_{\text{O}_2} = \sim 10\text{-}50$  mbar (the amounts of OKAO gas are a few times those in silicates). Every O<sub>2</sub> gas after exchange reaction was recovered at molecular sieve and measured for O isotope composition, followed by measurements of reacted silicates using the standard BrF<sub>5</sub> method with CO<sub>2</sub>-laser heating [6]. Some silicate runs were saved for petrological studies and future ion microprobe works.

**Results & Discussions:** Since we used relatively small amount of O<sub>2</sub> gas, isotopic compositions of both gas and solid changed after experiments. At high temperature equilibrium process, one can expect the reactants approaching to each other along near the mixing line connecting the initial compositions on a three-isotope plot, for example, slope  $\sim 0.75$  for Kainsaz and OKAO. However, run products of Allende, Kainsaz and Eagle station pallasite moved with much steeper slopes than those expected from a simple mixing. Compositions of the reacted OKAO gas fall on the right-side of the mixing line: in many case the  $\delta^{18}\text{O}$  values even increased. Similar results have been observed for ordinary chondrite samples. These behaviors can be explained by kinetic processes (evaporation and condensation) + mixing between liquid and gas. We suspect, during brief heating, some evaporated metallic irons recondensed as oxides preferentially with lighter oxygen in the gas. As a result, the reacted gas became heavier in its composition and the run products moved with much steeper slope than that of simple mixing. During chondrule and CAI forming heating events in the nebula, similar processes might have occurred to produce the chondritic mixing line.

**References:** [1] Clayton R. N. 1993. *Ann. Rev. Earth Planet. Sci.*, 21, 115-149. [2] Clayton R. N. 2002. *Nature* 415, 860-861. [3] Lyons J. R. & Young E. D. 2004. *Nature* 435, 317-320. [4] Yurimoto H. & Kuramoto K. 2004. *Science* 305, 1763-1766. [5] Yang Y. et al. 1995. *Geochim. Cosmochim. Acta*, 59, 2095-2104. [6] Kusakabe M. et al. 2004. *J. Mass Spec. Soc. Jpn.*, 52, 205-212.

**TRANSPORT IN THE SOLAR NEBULA: IMPLICATIONS FOR THE DEPLETION OF MODERATELY VOLATILE ELEMENTS IN CHONDRITIC METEORITES**

F. J. Ciesla<sup>1</sup> <sup>1</sup>Carnegie Institution of Washington, Department of Terrestrial Magnetism, 5241 Broad Branch Road NW, Washington, DC 20015. ciesla@dtm.ciw.edu

**Introduction:** The bulk abundances of moderately volatile elements (MOVEs, those elements that condense between ~650-1300 K) decrease with condensation temperature in many chondritic meteorites. Over the last 3+ decades, there have been two major theories for explaining this depletion trend: a two-component mixing model where volatile-rich and volatile-depleted materials were combined to form the chondritic meteorites [1] and an incomplete condensation model where solar nebular gas was continuously removed as the disk cooled [2]. As discussed in [3], the incomplete condensation model has gained favor, in part, due to the fact that astrophysical models of the solar nebula have been able to roughly reproduce the depletion trend [4,5]. Here I am using a more detailed model of transport in the solar nebula to evaluate whether such trends are still reproduced.

**Previous Work:** Cassen demonstrated that the incomplete condensation model could reproduce the MOVE-depletion observed in some chondrites [4,5]. In these models, the solar nebula was allowed to evolve, losing mass to the sun and expanding in radial extent to account for angular momentum transport. The nebula cooled as a result of its mass loss and coagulation of dust to form larger bodies. During this evolution, dust was transported through the disk by the net flow of the gas and was accreted by immobile planetesimals.

**This Work:** I have developed a model to re-examine whether incomplete condensation is consistent with astrophysical models of the solar nebula. In particular, I am focusing on the importance of those solids that are subjected to gas-drag migration, and therefore moved rapidly through the solar nebula. Cassen's models assumed that some fixed fraction of these bodies were lost to the sun [4,5]. However, recent work has shown that such bodies were either incorporated into planetesimals at heliocentric distances that differ from where these bodies formed or crossed evaporation fronts and lost their mass to the gas [6,7]. In either scenario, this transport led to spatial and temporal variations in the abundances of elements throughout the solar nebula. In addition, I also allow for the outward diffusion of MOVEs in the vapor phase. This work is based on a modified version of the transport model developed in [7].

**New Results:** Preliminary runs show that the redistribution of vapor by diffusion can lead to different results than those found in Cassen's models. For example, the outward diffusion of vapor can result in the *enhancement* relative to Si of MOVEs immediately outside the corresponding condensation front. This could imply that certain conditions were necessary for the incomplete condensation model to work or other processes are responsible for the observed MOVE depletions [3,8].

**References:** [1] Anders E. 1964. *Space Science Reviews* 3:583-714. [2] Wasson J. T. and Chou C.-L. 1974. *Meteoritics* 9:69-84. [3] Bland P. A. et al. 2005 *Publications of the National Academy of Sciences* 102:13755-13760. [4] Cassen P. 1996. *Meteoritics & Planetary Science* 31:793-806. [5] Cassen P. 2001. *Meteoritics & Planetary Science* 36:671-700. [6] Cuzzi J. N. and Zahnle K. J. 2004. *Astrophysical Journal* 614:490-496. [7] Ciesla F. J. and Cuzzi J. N. 2006. *Icarus* 181:178-204. [8] Alexander C. M. O. 2005. *Meteoritics & Planetary Science* 40:943-966.

### MULTIVARIATE ANALYSIS OF IN SITU AND EX SITU MARTIAN IMPACT GLASS.

B. A. Cohen, Institute of Meteoritics, University of New Mexico, Albuquerque NM 87131 ([bcohen@unm.edu](mailto:bcohen@unm.edu)).

Introduction: On the West Spur of Husband Hill, the Mars Exploration Rover Spirit encountered a class of rocks (Clovis class) thought to be extensively-altered clastic rocks of possible impact origin, having high Ni/Cr ratios and miniTES analyses distinguished by a component consistent with basaltic glass [1-4]. I am using multivariate analysis (multi-element correlations and principal component analysis) to try to determine whether a unique impact glass component can be characterized in these rocks, using the impact-generated Martian glass EETA79110 Lithology C as an analog. EETA79001 Lithology C: Lith C consists of pods of impact glass in a basaltic (Lith A) host and has been modeled as a mixture of 85% Lith A + 7% plagioclase + 8% Martian soil [5]. I used microprobe X-ray maps (Si, Mg, Ca, Ni, and S) of two Lith C pods. Principal component analysis shows that both pods have constant amount of S, regardless of Mg or Ca content, implying that S was introduced independently, not by specific sulfate or silicate phases. A weak anticorrelation of S with Si may reflect mechanical mixing of a small amount of soil (low Si) with the silicate minerals of Lith A (low S), as modeled by [5]. There was too much noise in the Ni element maps to make meaningful relationships with Ni; a longer integration time will be used to reduce noise in future efforts. A positive correlation between Mg and Ca (Principal Component 1) and a weak anticorrelation between Si and S (Principal Component 2) describe 55% of the total variation. Gusev rocks: Analyses using the same element set were performed using Athena APXS data (molar basis) of as-is, brushed, and RATted analyses of Adirondack- and Clovis-class rocks. Adirondack rocks are relatively unaltered basalts where RAT grinds penetrated thin weathering rinds. Analysis of the Adirondack class (n=17) shows that both S and Ni are strongly anticorrelated with Si, Ca, and Mg, showing that the components carrying these elements are distinguishable from the basalt. One principal component describes 80% of the variability among analyses, mainly describing an array with the RATted basaltic compositions at one end and a mix of brushed and as-is analyses along a trajectory enriched in S and Ni, as has been shown in [6], confirming these techniques. Preliminary analyses of the Clovis class (n=22) show that, unsurprisingly, this class of rocks is not as easily interpreted. Among these elements, Ca and S have the strongest positive correlation, demonstrating that S is carried in a sulfate phase [4] rather than primarily in an impact glass. However, in contrast to Adirondack rocks, Ni is positively correlated with Ca and anticorrelated with Si and Mg. Such a relationship might be expected if the precursor to the altered phases was an impact glass high in Ni. Such glasses may easily alter to phyllosilicates in the presence of water, as might be seen in the Clovis class rock Woolly Patch [7]. Further analysis of the Clovis class components is ongoing.

References: [1] Squyres, S.W., et al. (2006) JGR 111, doi:10.1029/2005JE002562. [2] Gellert, R., et al. (2006) JGR 111, doi:10.1029/2005JE002555. [3] Ruff, S.W., et al. (2006) in prep. [4] Ming, D.W., et al. (2006) JGR 111, doi:10.1029/2005JE002560. [5] Rao, M.N., et al. (1999) GRL 26, 3265. [6] McSween, H.Y., et al. (2004) Science 305, 842. [7] Wang, A., et al. (2006) JGR 111, doi:10.1029/2005JE002516.

**THE EFFECTS OF PERMEABILITY-DRIVEN WATER TRANSPORT ON THE EVOLUTION OF CM PARENT BODIES.** R.F. Coker<sup>1</sup>, B.A. Cohen<sup>2</sup>, P.A. Bland<sup>3</sup>. <sup>1</sup>Los Alamos National Laboratory, Los Alamos, NM 87545, USA (robc@lanl.gov); <sup>2</sup>University of New Mexico, Albuquerque NM 87131 USA; <sup>3</sup>Imperial College London, SW7 2AZ, UK.

**Introduction:** A range of numerical models of asteroid thermal evolution [1-4] predict large-scale movement of water on chondrite parent bodies. However, aqueous alteration in carbonaceous chondrites was likely isochemical [5], implying that little fluid flow occurred (see also Bland *et al.*, this conference). To resolve this contradiction, we have modelled the thermal evolution of CM parent bodies using three different expressions for permeability ( $k$ ).

We present models of CM parent bodies using a constant permeability of  $10^{-13} \text{ m}^2$  (representing lunar regolith) and two versions of the Blake-Kozeny-Carman (BKC) equation [6]. The first [7], based on micro-gravity experiments using mm-size balls, is valid only for small porosities and uses  $k = a^2 / 150 \times \phi^3 / (1-\phi)^2$ , where  $a$  is the grain size (in  $\mu\text{m}$ ) and  $\phi$  is the total porosity (the sum of voids and any liquid water). The second [8], based on experiments with calcite aggregates with a grain size of  $5 \mu\text{m}$ , uses  $k = a^2 / 2200 \times \phi^3$ .

**Results:** Since the unaltered matrix grain size for CCs is  $\sim 1 \mu\text{m}$  [9], we show in Fig. 1 the amount of  $\text{H}_2\text{O}$  moved upward through a given radius (compared to its initial  $\text{H}_2\text{O}$  mass) for  $a=0.5$  and  $5 \mu\text{m}$ . This model is for a 20 km diameter parent body that formed at 3 AU 1.5 Myr after the collapse of the solar nebula (CAI formation). The asteroid starts with 7% void space and 18% ice and a composition that results in 50% serpentine (by volume) after complete alteration. With a maximum total porosity of less than 30%, using the BKC expressions, the permeability for even  $a=5 \mu\text{m}$  is everywhere always less than  $10^{-13} \text{ m}^2$ . As a result, both water liquid and vapor transport is greatly reduced from previous models; in the models shown in Fig. 1, all  $\text{H}_2\text{O}$  transport is by water vapor. We discuss these and other results and their implications for CM parent body modelling.

**References:** [1] Grimm, R.E. and H.Y. McSween, Jr. (1989) *Icarus* 82, 244. [2] Travis, B.J. and G. Schubert (2005) *EPSL* 240, 234. [3] Coker, R.F. and B.A. Cohen (2001) *MAPS* 36, 43. [4] McSween, H.Y., Jr. *et al.* (2002) in *Asteroids III*, 559. [6] Hanowski, N.P. and A.J. Brearley (2001) *GCA* 65, 495. [7] Dullien, F.A.L. (1992) *Porous Media...* San Diego: Academic Press. [8] Yendler, B. and B. Webbon, *Capillary movement of liquid in granular beds*. 1993, SAE: Warrendale. p. 5. [9] Zhang, S., *et al.* (1994) *JGR* 99, 15741–15760. [10] Greshake, A. (1997) *GCA* 61, 437.

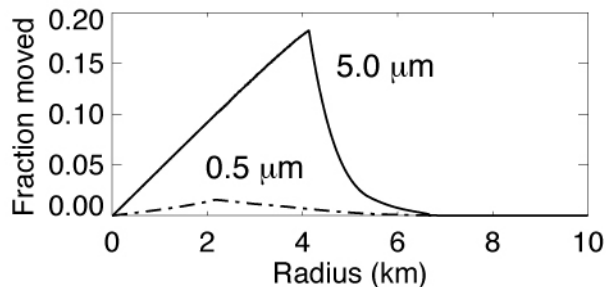


Fig. 1. Fraction of  $\text{H}_2\text{O}$  moved upward through each radius.

**RUBBLE PILES OR PLANETS? IMPLICATIONS FOR METEORITE PARENT BODIES.**

G. J. Consolmagno SJ<sup>1</sup> and D. T. Britt<sup>2</sup>. <sup>1</sup>Specola Vaticana, V-00120, Vatican City State. E-mail: gjc@specola.va <sup>2</sup>University of Central Florida, Orlando FL.

**Introduction:** Most meteorites show at least some degree of thermal, and in some cases aqueous, processing that presumably occurred on their parent bodies before they were ejected into Earth-crossing orbits. However, a detailed analysis of small bodies in the solar system indicates that virtually all bodies with masses less than  $10^{20}$  kg are today significantly porous, with many of them showing extensive macroporosity (>40%). It is not clear they could provide the physical environment needed to produce the observed degrees of metamorphism.

**Small Body Macroporosity:** Our previous work [1] has compared the densities of asteroids inferred via a number of methods to the densities of meteorites that are reasonable analogues to the surfaces of asteroids as inferred from their spectral features. The general trend is that all but the largest asteroids appear to be 20% to 50% or more macroporous, with a suggestion that C type asteroids tend to be more macroporous than S types. (Macroporosity here signifies the void spaces larger than the microcrack porosity seen in meteorite hand samples.) Data from recent spacecraft missions and new observations have allowed this analysis to be extended to cometary nuclei, additional small asteroids, planetary satellites, (especially using Cassini measurements of the densities of Saturn's moons), and Centaurs and Transneptunian objects, where we have estimated densities from their shape and spin characteristics [2]. From this analysis we find a general trend that, regardless of composition, bodies larger than  $10^{20}$  kg mass tend to be well-compacted objects while smaller bodies, down to fragments much smaller than a few hundred meters diameter, are either extensively fragmented or loose piles of rubble. The universal nature of this size limits suggests that it may reflect an underlying physics, either that such-sized bodies are able to withstand catastrophic disruptions or that they are able to reshape themselves after such disruptions.

**Implications for Meteorite Parent Bodies:** Much of the new data included in this analysis comes from recent spacecraft missions, which allow us not only to measure the bodies' densities but also inspect images of their surfaces. Not surprisingly, the rubble pile surfaces are characterized primarily by dust, rubble, and impact features; even their occasional tectonic features appear to be related to impact or accretion events. On the other hand, more complex geologic processes (including heating and alteration of surface materials) can be seen on larger icy moons and inferred for larger asteroids like Ceres and Vesta [3, 4]. This suggests that either only large meteorite parent bodies are capable of producing metamorphosed meteorites and aqueous alteration, or that such metamorphism occurred very early in solar system history before smaller coherent bodies were fragmented and reaccreted.

**References:** [1] Britt D. T. et al., 2002 *Asteroids III* (W. Bottke and R. Binzel, eds.), Univ. of Arizona Press, Tucson; pp 485-500. [2] cf. Britt D. T. et al. (2006), Abs. #2214, LPSC XXXVII; Consolmagno G. J. et al., (2006) Abs. #1222, LPSC XXXVII; [3] Thomas et al., (2006), Abs. #1639, LPS XXXVII. [4] Thomas P. et al., (2005) *Nature* 437: 224.

### MASS-DEPENDENT FRACTIONATION OF NICKEL ISOTOPES IN IIIAB IRON METEORITES.

D. L. Cook<sup>1,2,3</sup>, M. Wadhwa<sup>2,3</sup>, R. N. Clayton<sup>1,2,4</sup>, P. E. Janney<sup>2,3</sup>, N. Dauphas<sup>1,2,4</sup>, and A. M. Davis<sup>1,2,4</sup>. <sup>1</sup>Dept. of the Geophysical Sciences, The University of Chicago, Chicago, IL 60637 (dave-cook@uchicago.edu). <sup>2</sup>Chicago Center for Cosmochemistry, Chicago, IL 60637. <sup>3</sup>Dept. of Geology, The Field Museum, Chicago, IL, 60605. <sup>4</sup>Enrico Fermi Institute, The University of Chicago, Chicago, IL, 60637.

**Introduction:** Studies of the mass-dependent fractionation of stable isotopes of light elements have been a useful tool for investigating early solar system processes operating in the nebula and on parent bodies. The advent of multi-collector ICPMS has expanded the range of elements now available for such investigations. Studies of Fe, Cu, and Zn isotopes in meteorites [*e.g.* 1,2] show that the transition metals underwent mass-dependent fractionation during processes occurring in the early solar system. Additionally, Ni isotopes in metal from various meteorite groups follow a mass-dependent fractionation trend [3]. Nevertheless, the mass-dependent fractionation of Ni isotopes in natural samples remains largely unexplored. We have chosen to examine the possible effects on the isotopic composition of Ni due to fractional crystallization of a liquid Fe-Ni alloy during core formation by investigating a suite of the magmatic IIIAB iron meteorites.

**Samples:** Relatively large ( $\approx 1$  g) pieces of IIIAB metal were digested by [4] for their Fe isotope study. Thus, digested but chemically unprocessed solutions remained for many samples, and aliquots of these solutions were used to investigate Ni isotopic fractionation in IIIAB irons. Samples were chosen to represent a wide range in Ni content, which is considered a proxy for the degree of fractional crystallization. Specifically, Fe-Ni metal from the following IIIAB irons was analyzed: Avoca, Augustinovka, Bald Eagle, Bella Roca, Henbury, Nova Petropolis, Orange River Iron, and Welland.

**Results and Discussion:** Five of the IIIAB irons investigated here (Avoca, Augustinovka, Henbury, Nova Petropolis, and Orange River Iron) have similar Ni isotopic compositions and yield a weighted average value of  $0.48 \pm 0.12$   $\epsilon$  per a.m.u. relative to the SRM 986 Ni standard. The other three samples (*i.e.*, Bald Eagle, Bella Roca and Welland) are enriched in the heavy isotopes of Ni and have compositions ranging from 1.44 to 2.93  $\epsilon$  per a.m.u. However, the degree of mass fractionation of Ni isotopes does not correlate with the Ni content ( $r^2 = 0.11$ ). This suggests that if all IIIAB irons originated in a single parent body, core formation and crystallization did not mass fractionate Ni isotopes in a systematic way. In fact, fractionation of Ni isotopes in different IIIAB iron meteorites may be the result of a combination of factors including partitioning between metal and silicate during core segregation and the interaction of a metallic melt with a sulfide melt during core crystallization.

**Acknowledgement:** We thank E. Mullane for generously providing digested aliquots of the IIIAB samples studied here.

**References:** [1] Zhu X. K. et al. 2001. *Nature* 412: 311-313. [2] Luck J.-M. et al. 2005. *Geochimica et Cosmochimica Acta* 69: 5351-5363. [3] Moynier F. et al. 2004. Abstract #1286. 35<sup>th</sup> Lunar and Planetary Science Conference. [4] Mullane E. et al. 2005. *Meteoritics & Planetary Science* 40: A108.

**Mg ISOTOPES FRACTIONATION IN MELILITE IN AN ALLENDE TYPE-A INCLUSION: A HIGH-PRECISION, HIGH-SPATIAL RESOLUTION APPROACH.**

M. Cosarinsky<sup>1</sup>, K. D. McKeegan<sup>1</sup>, I. D. Hutcheon<sup>2</sup> and S. Fallon<sup>2</sup>. <sup>1</sup>Dept. Earth & Space Sciences, UCLA, Los Angeles, CA 90095-1567; <sup>2</sup>Chemical Biology & Nuclear Science Division, Lawrence Livermore National Laboratory, Livermore, CA 94551-0808. mariana@ess.ucla.edu.

**Introduction:** Type A CAIs are coarse-grained, melilite-rich inclusions common in CV chondrites. The irregular and nodular structures of some of these CAIs, in addition to their chemical compositions, suggest an origin by condensation and aggregation rather than melting [1]. Previous isotopic studies have shown that these objects are highly heterogeneous in their stable Mg isotope records [2]. In order to better understand the microdistribution of Mg isotopes in these samples we performed coordinated high precision (ims1270) and high spatial resolution (NanoSIMS) ion microprobe analyses on melilite and spinel in an Allende type-A CAI.

**Results and Discussion:** Allende TS25 is a large (15 x 5 mm), oblong, coarse-grained type-A CAI consisting of reversely zoned melilite crystals ( $\text{\AA}_{k_{25}}$  in the core to  $\text{\AA}_{k_{10}}$  near the rim) with inclusions of spinel, hibonite, and perovskite. Spinel grains are mostly euhedral, 10-15  $\mu\text{m}$  in size, and sometimes occur grouped in clusters. Alteration minerals are abundant, especially around the perimeter of the CAI or where it is fractured. A well-developed and continuous Wark-Lovering rim (WLR, [3]) surrounds the inclusion [2]. The same WLR sequence also occurs inside the inclusion as "enclosed" features, usually lining interior cavities or brecciated fragments. The enclosed WLRs are usually less altered as is the melilite right below these rims. Mg isotope analyses show large ranges in fractionation in melilite ( $^{25}\text{Mg} = -2.5$  to  $+16.4$  ‰,  $1 \pm 0.3$ ) and spinel ( $^{25}\text{Mg} = -1.4$  to  $+23.7$  ‰,  $1 \pm 0.1$ ). NanoSIMS data yield consistent ranges in  $^{25}\text{Mg}$  values. The data are correlated in the sense that the most fractionated spinel grains occur within fractionated melilite and those interior melilite grains that do not show isotopic enrichments contain inclusions of isotopically normal spinel. Analyses of these phases near the WLR yield  $^{25}\text{Mg}$  compositions closer to normal (unfractionated). In particular, melilite adjacent to WLR spinel is the lightest. High spatial resolution analyses show a progressive variation in  $^{25}\text{Mg}$  towards the rim of the order of 14 ‰ over 100  $\mu\text{m}$ , with only a slight chemical gradient of decreasing Mg contents ( $\text{\AA}_{k_{8-1}}$ ).

Our data suggest that Allende TS-25 formed by the aggregation of grains with different nebular histories that then underwent minor melting or solid-state recrystallization without major isotopic equilibration. The petrographic correlation between isotopically heavy spinel and melilite indicates that some diffusive exchange from spinel into melilite occurred [4]. In addition, the strong compositional gradient observed close to the WLR suggests that isotopically heavy melilite exchanged with the ambient nebular gas, but the preservation of the fine-scale isotopic heterogeneities implies that heating was brief followed by cooling rates sufficient to allow for some diffusive transport of Mg between spinel and melilite and between melilite and the gas.

**References:** [1] MacPherson G.J. and Grossman L. (1984) *GCA* **48**, 29-46; [2] Cosarinsky et al. (2005) *LPSC* **36**, #2105 (abstract); [3] Wark D. and Boynton W.V. (2001) *MAPS* **36**, 1135-1166; [4] Sheng et al. (1992) *GCA* **56**, 2535-2546.

**THERMAL PROCESSES OF THE 4 Kyr BP OCEANIC IMPACT BASED ON CARBON AND MINERAL PHASE ASSOCIATION IN MELT PRODUCTS.**

M.-A. Courty<sup>1</sup>, B. Deniaux<sup>1</sup>, A. Crisci<sup>2</sup>, K. Grice<sup>3</sup>, P. Greenwood<sup>3</sup>, M. Mermoux<sup>2</sup>, D. Smith<sup>4</sup>, M. Thiemens<sup>5</sup>. <sup>1</sup>UMR 5198, CERP 66720 Tautavel, France, [courty@tautavel.univ-perp.fr](mailto:courty@tautavel.univ-perp.fr). <sup>2</sup>LPMI-ENSEEG, Univ. Grenoble, 38042 Saint-Martin d'Hères, France. <sup>3</sup>Curtin Univ. Technology, Perth, WA, 6845, Australia. <sup>4</sup>MNHN-Minéralogie, 59 rue Buffon, 75005 Paris, France. <sup>5</sup>Chemistry and Biochemistry, Univ. California, San Diego 92093, USA.

**Introduction:** Impact events into crystalline targets are known to generate high pressure shock and large volumes of melt rocks and glasses [1]. In contrast, impacts into volatile-rich soft sediments lead to minor melt formation, weak shock effects and high ejecta dispersion [2]. Thus, the related-impact signature mainly results from thermal effects during collision and ejecta redistribution [3]. The well preserved worldwide ejecta-strata horizon of the 4 kyr BP impact [4] provides a unique opportunity to understand impact-thermal processes.

**Methods:** The 4 kyr BP impact products were compared from marine and terrestrial records. The key-association of nano-diamonds, graphite and hydrocarbons in melt clasts and in the host materials was studied using an environmental SEM/EDAX microprobe, Raman micro-spectrometry, electron microprobe, TEM, GC-IR-MS and isotope analysis (C, O, S, Pb, Fe, Cr).

**Results and discussion :** The ca. 7 m thick sequence in deep sea cores along the Antarctica coast showing impact-melt clasts with heated marine sediments provides stratigraphic and geochemical signatures to identify the proximal ejecta from an oceanic impact. The impact debris show devitrified melt clasts with crystalline defects due to hydrocarbon incorporation before quenching. Metallic droplets associated to high temperature graphite and clusters of nano-diamonds form splash mounds on the melt clasts and on heated marine particles. In contrast, the distal impact-ejecta debris display sharp contact of weakly heated marine clasts with vesicular flow-textured glass derived from marine sediments. Thermal transformations of the host soil surface splashed by the distal impact-ejecta express pulverisation of a volatile-rich carbonaceous melt. Metal-rich clasts with a banded texture formed of graphitic and alumino-silicate sheets are fragments of the projectile, possibly a CV3 carbonaceous chondrite. Metallic mounds in the distal-impact glass formed in situ from local vaporization of the projectile fragments. Clusters of HT graphite, nano-diamonds and hydrocarbons coating voids in the impact glass are also vaporization residues of the projectile. Absence of projectile clasts in the proximal ejecta-debris would result from its total vaporization in the collision zone. In contrast preservation of projectile clasts in the distal dispersion area would express its fragmentation while crossing the Earth-atmosphere and block- entrainment after the collision by the impact ejecta while rising.

**References:** [1] Dressler B.O. and Reimold W.U. 2001. *Earth-Science Reviews* 56: 205-284. [2] Kieffer S.W. and Simons C.H. 1980. *Rev. Geophys. Space Phys.*, 18: 143-181. [3]. Wasson J.T. 2003. *Astrobiology*, 3(1): 163-179. [4]. Courty M.A. et al. 2006. *Geophys. Res. Abst.* A01812.

**A SEARCH FOR EXTRATERRESTRIAL CHROMITE  
ACROSS THE CRETACEOUS-PALEOGENE BOUNDARY  
AT GUBBIO, ITALY.**

A. Cronholm and B. Schmitz. Department of Geology, Lund University, SE-22362 Lund, Sweden. E-mail:

Anders.Cronholm@geol.lu.se; Birger.Schmitz@geol.lu.se.

The distribution of sediment-dispersed extraterrestrial chromite (EC) grains ( $>63 \mu\text{m}$ ) has been studied in marine, condensed limestone across the Cretaceous-Paleogene (K-P) boundary in the Bottaccione Gorge section at Gubbio, Italy. Chromite is a common accessory mineral in ordinary chondrites [1] and is highly resistant to weathering. Hence, chromite is often the only surviving mineral of decomposed meteorites, making it useful for assessing the accretion rates of extraterrestrial material in ancient sediments [2, 3]. The EC can be readily distinguished from terrestrial chromite based on its element composition, including specific ranges of  $\text{TiO}_2$  (2.0-3.5 wt%) and  $\text{V}_2\text{O}_3$  (0.6-0.9 wt%) [4]. The aim of this study is to determine if the K-P boundary asteroid impact was associated with an enhanced influx to Earth of ordinary chondritic meteorites.

Six limestone samples of 28 kg each and one of 14 kg were collected from 7.2 m below the K-P boundary clay to 17.2 m above it. Three of the samples were taken at or close to the K-P boundary, while the remaining constituted background material. The samples were leached in HCl and HF. Chromite grains ( $>63 \mu\text{m}$ ) were picked from the residues and analyzed by EDS methods [2, 3].

In a total of 182 kg of limestone only four EC grains were found ( $0.022 \text{ EC grains kg}^{-1}$ ). Based on estimated sedimentation rates for the Gubbio section [5], we calculate a flux of  $\sim 0.23 \text{ EC grains m}^{-2} \text{ kyr}^{-1}$ . The four grains were found throughout the section, and no increase of EC grains could be observed in the samples from the K-P boundary. The absence of EC grains at the K-P boundary is not surprising considering that the K-P impactor probably was a carbonaceous chondrite low in chromite [6, 7]. Our results give no support for the K-P impactor being related to perturbations of the asteroid belt during chaotic transitions in the motion of the inner planets, see [8].

The content of EC grains in the Gubbio limestone is very low compared to Middle Ordovician limestone from Kinnekulle, southern Sweden. The latter sediment contains 1-3 EC grains per kg, which has been interpreted as a two-orders-of magnitude increase in the influx of ordinary chondrites to Earth following the disruption of the L chondrite parent body  $\sim 470 \text{ Ma}$  [2-4]. Sedimentation rates of the limestones at Kinnekulle and Gubbio lie at the same order of magnitude [3, 5], i.e. a few mm per thousand years. At Kinnekulle condensed limestone that formed prior to the L chondrite disruption event show similarly low EC content ( $5 \text{ EC grains } 379 \text{ kg}^{-1}$  or  $0.013 \text{ EC grains kg}^{-1}$ ) as the Gubbio limestone [3]. These low concentrations of EC grains probably reflect the normal flux of ordinary chondrites to Earth.

**References:** [1] Rubin A. E. 1997. *Meteoritics & Planetary Science* 32:231-247. [2] Schmitz B. et al. 2003. *Science* 300:961-964. [3] Schmitz B. and Häggström T. 2006. *Meteoritics & Planetary Science* 41:455-466. [4] Schmitz B. et al. 2001. *Earth and Planetary Science Letters* 194:1-15. [5] Mukhopadhyay S. et al. 2001. *Geochimica et Cosmochimica Acta* 65:653-669. [6] Shukolyukov A. and Lugmair G. W. 1998. *Science* 282:927-930. [7] Kyte F. T. 1998. *Nature* 396:237-239. [8] Varadi et al. 2003. *Astrophysical Journal* 592:620-630.

**FIRST SYSTEMATIC TEM/NANOSIMS COORDINATED STUDY OF CRYSTAL STRUCTURE AND ISOTOPIC COMPOSITION OF PRESOLAR SILICON CARBIDE**

T. L. Daulton<sup>1,2</sup>, F. J. Stadermann<sup>3,2</sup>, T. J. Bernatowicz<sup>3,2</sup>, S. Amari<sup>3,2</sup>, and R. S. Lewis<sup>4</sup>. <sup>1</sup>Center for Materials Innovation, <sup>2</sup>Physics Department, <sup>3</sup>Laboratory for Space Sciences, Washington University in St. Louis, St. Louis MO 63130, USA. <sup>4</sup>Enrico Fermi Institute, University of Chicago, Chicago IL 60637, USA.

**Introduction:** Submicron- to micron-sized presolar grains of SiC are ubiquitous in the matrices of primitive chondrites. While numerous studies have measured the isotopic compositions in primary and trapped elements of individual presolar SiC grains [1], providing information on their stellar sources, there have been few detailed studies of their microstructure. Grain microstructures provide important information on mechanisms of grain formation, physical conditions at sources of formation, and metamorphic processing subsequent to formation. The value of isotopic and microstructural measurements on presolar SiC grains would be increased if those data sets were correlated to one another on an individual grain basis.

**Results:** Suspensions of SiC isolated by acid dissolution from Murchison (KJB residue) [2] were deposited on transmission electron microscopy (TEM) grids. Crystal structure of randomly selected grains was determined by TEM; three SiC polytypes or stacking sequences (cubic 3C, hexagonal 2H, and disordered) along with their intergrowths and a range of defect and twin microstructures were identified [3,4]. The locations on the TEM grid of 48 TEM-characterized grains of the following structure types, hexagonal 2H SiC (3% of Murchison SiC population); intergrowths of cubic 3C and hexagonal 2H SiC (17% of population); and disordered SiC (1% of population), were determined for use in subsequent isotopic measurement by NanoSIMS.

Forty randomly selected grains on the TEM mount, presumably mostly 3C SiC (79% of population), were analyzed by NanoSIMS as a control, and they exhibited a range of isotopic compositions similar to those measured in far larger presolar SiC populations [1]. As a group, the 2H, 2H/3C intergrowth, and disordered SiC structure types are isotopically anomalous and exhibit a greater scatter in both  $\delta^{29}\text{Si}$  and  $\delta^{30}\text{Si}$  in comparison to the predominantly 3C SiC set of randomly selected grains. All three measured 2H grains are isotopically mainstream. Of the 42 SiC 2H/3C intergrowth grains analyzed, one has  $^{12}\text{C}/^{13}\text{C} = 8.7 \pm 0.8$  (i.e.,  $< 10$ ) and is identified as type A+B; two exhibit small enrichments in  $^{28}\text{Si}$  and are possibly type X; one has  $^{12}\text{C}/^{13}\text{C} = 110.3 \pm 2.3$  (i.e.,  $> 100$ ) with Si isotopes on the  $^{30}\text{Si}$ -enriched side of the mainstream distribution and is identified as type Y; two have mainstream  $^{12}\text{C}/^{13}\text{C}$  with Si isotopes on the  $^{30}\text{Si}$ -enriched side of the mainstream distribution as well as  $\delta^{29}\text{Si} < 0$  and are identified as type Z. We also confirm our earlier inference that one-dimensionally disordered SiC [3,4] is a presolar grain type. Interestingly, all three disordered grains analyzed have very similar isotopic compositions in  $\delta^{29}\text{Si}$  (46 to 63‰),  $\delta^{30}\text{Si}$  (34 to 57‰), and  $^{12}\text{C}/^{13}\text{C}$  (51 to 60). Although the statistics are limited, the probability of three disordered grains clustering as observed in Si isotopes is  $< \sim 3\%$ , suggesting disordered SiC might be associated with a specific type of stellar source.

**References:** [1] Meyer B. S. and Zinner E. 2006. in *Meteorites and the Early Solar System II*, Lauretta D. and McSween Jr. H. Y. (eds) U. of Arizona Press. [2] Amari S. et al. 1994. *GCA* 58, 459-470. [3] Daulton T. L. et al. 2002. *Science* 296, 1852-1855. [4] Daulton T. L. et al. 2003. *GCA* 67, 4743-4767.

## THEORY OF ISOTOPIC FRACTIONATION DURING PHASE GROWTH IN A DIFFUSION-LIMITED REGIME.

N. Dauphas<sup>1</sup>. <sup>1</sup>Origins Laboratory, Department of the Geophysical Sciences and Enrico Fermi Institute, The University of Chicago, 5734 South Ellis Avenue, Chicago IL 60637. E-mail: dauphas@uchicago.edu

**Introduction:** Phase growth in a diffusion-limited regime is a ubiquitous process in planetary sciences. It may for instance apply to growth of hematite spherules from an aqueous fluid on Mars. Such a process can affect isotopes in two ways. (i) Phase growth creates a concentration gradient between the surface and the surrounding medium. Different isotopes have slightly different diffusion coefficients. They therefore can be supplied at different rates to the surface of the growing phase. (ii) If there is any equilibrium or kinetic isotope fractionation at the interface between the two phases, diffusion will control whether this fractionation is expressed in the fluid or in the solid. Frank [1] and Berner [2] evaluated the influence of supersaturation at infinity on the rate of crystal and concretion growth in a diffusion-limited regime. Recently, Dauphas and Rouxel [3] extended this work to calculate isotopic fractionation in the growing phase.

**Results:** The intuitive idea regarding the dynamic of this process might be that when the system has reached steady state, the interface grows linearly with time and there can be no isotopic fractionation because whatever comes in must be incorporated in the growing phase. This picture is flawed however because what governs the supply of elements to the growing phase is diffusion. If the concentration of an element is to remain constant at the interface (at saturation), then the interface must move as  $\sqrt{t}$  [1,2]. The differential equations governing diffusion transport of elements towards a growing sphere or an infinite plate can be solved analytically when the interface moves as  $\sqrt{t}$  (quasi-stationary solution). The transient state for an initial step-function in concentration was calculated by numerical integration using the front-tracking fixed finite-difference grid method described by Crank [4]. The degree of supersaturation at infinity compared to the surface ( $C_{sat}^* = C_{sat}/C_\infty$ ) is a convenient nondimensional variable to describe the system. When  $C_{sat}^*$  is close to 1, then the concentration gradient is small, the phase grows slowly, there is no isotopic fractionation due to diffusion, but the fractionation at the interface is expressed in the growing phase. When  $C_{sat}^*$  is close to 0, the phase grows rapidly, the isotopic fractionation due to diffusion is maximal, but the fractionation at the interface is expressed in the source medium.

**Conclusions:** Phase growth in a diffusion-limited regime can fractionate isotopes. At high growth rates, isotope fractionation will occur because of differences in diffusivities of different isotopes. At low growth rates, kinetic or equilibrium isotope fractionation at the interface will be expressed in the growing phase. The formalism described here may be useful for understanding and predicting isotopic fractionation measured in a variety of planetary materials, including terrestrial analogues of martian blueberries [5].

**References:** [1] Frank F.C. 1950. *Proc Roy Soc London* A201:586-599. [2] Berner R.A. 1968. *Geochim Cosmochim Acta* 32:477-483. [3] Dauphas N., Rouxel O. 2006. *Mass Spectrometry Reviews* 25:515-550. [4] Crank J. 1984. *Free and moving boundary problems*. Oxford: Oxford University Press. [5] Busigny V., Dauphas N. 2006. *Earth Planet Sci Lett*, submitted.

### QUANTITATIVE MAPPING OF MELILITE ELEMENTAL COMPOSITION IN REFRACTORY INCLUSIONS.

A. M. Davis, Department of the Geophysical Sciences, Enrico Fermi Institute and Chicago Center for Cosmochemistry, University of Chicago, Chicago, IL 60637 (a-davis@uchicago.edu).

**Introduction:** Compositional variations in minerals in rocks are typically depicted in a qualitative way through x-ray maps and in a quantitative way through plots of concentration vs. distance along linear profiles. The utility of x-ray maps has been improved in recent years through the application of combined color elemental maps [e.g., 1]. Modern x-ray microanalysis hardware and software also allow quantitative mapping to be done. Here, an x-ray spectrum is collected at each pixel and reduced to provide a chemical analysis. The information from quantitative maps can be extracted and manipulated so that maps of mole % of mineral components in solid solutions series can be produced. Several such maps for melilite have been published recently, but the methods used have not been described in detail.

**Methods:** All maps were collected using a JEOL JSM-5800LV SEM with an Oxford Link ISIS-300 microanalysis system. Maps are collected at a beam current high enough to produce ~40,000 counts per second on the detector, typically 10 nA, with a dwell time of 1–2 s per pixel. For mapping melilite, quantitative maps of wt% MgO, Al<sub>2</sub>O<sub>3</sub>, SiO<sub>2</sub> and CaO are needed. The Oxford software allows export of the data in each of these elemental maps as a grid of concentrations, along with grids of the 1 $\sigma$  uncertainty for each element. After conversion of each grid to a column of numbers, plots of uncertainty vs. concentration are used to eliminate pixels that are in cracks or on epoxy. Such data points will have anomalously high uncertainties. Once errant data points are eliminated, the mole percent åkermanite is calculated for each spot. Spots that are not melilite can easily be recognized and eliminated, as the Åk content based on Mg will not agree with that based on Al or Si. After culling of data in cracks and for minerals other than melilite, the mole % Åk data is transformed back to grid form and plotted as a color intensity map using the software package Igor. Collection and treatment of data using methods described here gives precision of ~1 mole % Åk.

**Applications:** Åk mapping led to the discovery of extreme variations in melilite composition in the unusual Allende inclusion Golfball, where the entire range of melilite composition from Åk<sub>2</sub> to Åk<sub>72</sub> can be found only  $\mu\text{m}$  apart [2]. A recent study of experimental crystallization of melilite from CAI melts led to the discovery of sector-zoned melilite [3]. Sudden jumps of a few mole % Åk along linear profiles through melilite in natural CAIs may be due to sector-zoning rather than complicated growth history. Given the bulk compositions of Type B CAIs in CV chondrites, the most Åk-poor melilite expected to crystallize contains 15–25 mole % Åk. However, most Type B CAIs have more gehlenitic compositions, sometimes as low as Åk<sub>1</sub>, within 100  $\mu\text{m}$  of the rim. This has been known in a qualitative way from polarized light microscopy for some time, but Åk mapping makes this very easy to see. This unusual zoning feature likely results from a heating event subsequent to crystallization and may be related to Wark-Lovering rim formation.

[1] Krot A. N. et al. 2003. In *Meteorites, Planets, and Comets* (Ed. A. M. Davis), Vol. 1 *Treatise on Geochemistry* (Eds. H. D. Holland and K. K. Turekian), Elsevier-Pergamon, Oxford, pp. 407–430. [2] Simon S. B. et al. 2005, *Meteoritics & Planetary Science* 40: 461–475. [3] Mendybaev R. A. et al. 2006, *Geochimica et Cosmochimica Acta* 70: 2622–2642.

**THERMAL ANNEALING OF AMORPHOUS SILICATES:  
THE BEHAVIOUR OF SILICATE DUST IN  
PROTOPLANETARY DISCS**

C. Davoisne<sup>1</sup>, Z. Djouadi<sup>2</sup>, H. Leroux<sup>1</sup>, L. d'Hendecourt<sup>2</sup>, A. P. Jones<sup>2</sup> and D. Deboffle<sup>2</sup>. <sup>1</sup> Laboratoire de Structure et Propriétés de l'Etat Solide (LSPES) USTL, 59655 Villeneuve d'Ascq, France. E-mail: [carine.davoisne@ed.univ-lille1.fr](mailto:carine.davoisne@ed.univ-lille1.fr). <sup>2</sup> Institut d'Astrophysique Spatiale (IAS), Bâtiment 121, F-91405 Orsay, Université Paris-Sud 11-CNRS (UMR 8617) France.

**Introduction:** In protoplanetary discs, the infrared spectra from ISO have shown evidence for crystalline silicate features [1] whereas in the interstellar medium, all the silicate dust is detected in an amorphous state [2]. To explain the presence of crystalline silicates in protoplanetary discs, condensation and thermal annealing are frequently invoked [3, 4]. In this study we explore the behavior of amorphous ferromagnesian-silicates under annealing at controlled atmosphere, with the aim to precise the microstructural evolution of the interstellar precursors in the inner protoplanetary disc.

**Experimental procedure:** The amorphous silicate precursor (olivine composition  $Mg_{1.8}Fe_{0.2}SiO_4$ ) was obtained by electron beam evaporation as 100 nm thick films onto different substrates [5]. The thin films were then submitted to thermal annealing in situ in a transmission electron microscope (TEM) or in a furnace under vacuum at controlled atmosphere ( $O_2$ ,  $CO/CO_2$  and  $C/CO$  buffers).

**Results:** Under reduced conditions we have observed the formation of spherical iron metallic precipitate near 600°C and their development at higher temperature. A progressive recrystallization of the silicate film into Mg-rich silicates (forsterite and enstatite) is obtained for temperature above 700°C.

The investigation of microstructure after thermal annealing under oxidized conditions shows the formation of an Mg-Fe oxide (magnesioferrite) at 700°C. The matrix recrystallizes progressively for temperature above 700°C into Mg-rich silicate (forsterite and enstatite).

**Conclusion:** These results demonstrate that the microstructural evolution under thermal annealing is strongly dependent on the gas composition in which the silicate dust recrystallizes.

The crystalline phases formed are in strong agreement with those (principally Mg-rich silicate) observed by ISO in the protoplanetary discs and some of the microstructures can be related to those in IDPs, the so-called GEMS. Our results suggest a formation of these different phases in reduced conditions and are compatible with the scenario of a recrystallization of interstellar dust by thermal effect in protoplanetary discs. By means of a turbulent effect the annealed silicates can then be redistributed in the region of formation of comet and meteorite [6, 7].

**References:** [1] Malfait et al. 1998. *Astronomy & Astrophysics* 332: L25-L28. [2] Li A. and Draine B. T. 2001. *Astrophysical Journal* 550:L213-L217. [3]. Rietmeijer F. J. M. 2004. Abstract #1960. 35<sup>th</sup> Lunar and Planetary Science Conference [4] Keller L. P. and Messenger S. 2004. Abstract #1985. 35<sup>th</sup> Lunar and Planetary Science Conference. [5] Djouadi Z. et al. 2005. *Astronomy & Astrophysics* 440: 179-184. [6] Bockelée-Morvan D. et al. 2002. *Astronomy & Astrophysics* 384: 1107-1118. [7] Davoisne C. et al. 2006. *Astronomy & Astrophysics* 448: L1-L4.

### CAN THE WATER PRESSURE IN THE ACCRETION DISK SUSTAIN WATER ADSORPTION ON OLIVINE?

N.H. de Leeuw<sup>1</sup>, M. Stimpff<sup>2</sup>, C.R.A. Catlow<sup>1</sup>, M.J. Drake<sup>2</sup>, P. A. Deymier<sup>3</sup> and A. W. Walker<sup>4</sup>. <sup>1</sup>Department of Chemistry, University College London, UK; <sup>2</sup>Lunar and Planetary Laboratory, University of Arizona, Tucson, <sup>3</sup>Department of Material Science and Engineering, University of Arizona, Tucson, <sup>4</sup>University of Cambridge, Cambridge, UK

**Introduction:** In the accretion disk, gases coexist with solid particles for long periods. According to thermodynamic calculation the H<sub>2</sub>O/H<sub>2</sub> ratio in the accretion disk, was about 5x10<sup>-4</sup>, [1] which correspond to a p<sub>H<sub>2</sub>O</sub> of ~ 10<sup>-8</sup>bar. Note that the equilibrium partial pressure is probably a lower limit [2 -3]. Astronomical observations show that dust clouds consist of Mg-rich olivine (Mg<sub>2</sub>SiO<sub>4</sub>, aka forsterite), pyroxenes and other refractory minerals with radii <1μm [4]. Several authors [5-7] suggest that these refractory minerals should coalesce during the early stage of planet formation by means of low-velocity impacts that would create low-density, irregularly shaped fractal structures. The concomitant presence of small fractal particulates with high surface area and of water gas in an environment of low-energy impacts raises the overlooked question of the role of adsorption of water into the building blocks of the rocky planets.

**Methods:** We have employed atomistic simulation techniques (program GULP [8-9]), to study the interaction between selected forsterite surfaces and water gas. We simulated associative adsorption, which entails molecular adsorption of a water molecule over olivine surfaces [10] while [11] simulated dissociative adsorption of water (adsorption of dissociated water molecules) over the same surfaces and investigated the energetic for both partial and total coverage.

The process of adsorption can be described according to the following equation: Surface + H<sub>2</sub>O(g) ↔ Surface\*(H<sub>2</sub>O), where the left hand side of the equation represents water adsorbed on the surface. Once the thermodynamic properties of the reaction are known, the p<sub>H<sub>2</sub>O</sub> required to adsorb water on the forsterite surfaces at the T of interest can be obtained.

**Results:** Our calculations show that adsorption of water can take place on perfect forsterite surfaces at temperatures consistent with the inner accretion disk. In particular, associative adsorption on the {100} surface can begin at ~ 700K, while dissociative adsorption can take place on several surfaces at temperatures as high as 1000K. Our investigation shows that adsorption of water gas onto forsterite grains is consistent with temperatures in the accretion disk. Next, we will explore the effect of olivine composition on the efficiency of adsorption and the kinetics of such reaction by means of Molecular Dynamic calculation.

**References:** [1] Lodders K. 2003. *The Astrophysical Journal* 591:1220-1247. [2] Clayton R.N. 2004 LPI Contribution 1203, 16. [3]Cuzzi J.N. et al. 2004. LPI Contribution 1218.[4] Boekel R.V. et al. 2004. *Nature* 432:479-481. [5] Weidenschilling S.J. et al. 1999. *Protostar and Planets III*, UofA Press, 1031-1060. [6] Blum J. et al. 2000. *Icarus* 143:138-146. [7] Fogel M. et al. 1998. *The Astrophysical Journal* 501 :175-191. [8] Gale J.D. et al. 2003. *Molecular Simulation* 29:219-314. [9] Gale J.D. 1997. *Journal of the Chemical Society Faraday Transactions* 93:629-637. [10] Stimpff M. et al. 2006. *Journal of Crystal Growth* accepted for publication. [11] de Leeuw N.H. et al. 2000. *Physics and Chemistry of Minerals* 27:332-341.

### MANGANESE-RICH PHASES IN CM CHONDRITES: MN-CR SYSTEMATICS OF CARBONATES AND SILICATES.

Simone de Leuw<sup>1</sup>, Alan E. Rubin<sup>1</sup> and John T. Wasson<sup>1</sup>.  
<sup>1</sup>Institute of Geophysics and Planetary Physics, University of California, Los Angeles, CA 90095-1567, USA. E-mail: sdeleuw@ucla.edu.

**Introduction:** CM carbonaceous chondrites record a variety of nebular and parent-body processes. An important process that affected CM chondrites is aqueous alteration. This process resulted in the formation of secondary phases [1, 2]. Little is known about the timescale and locations of these alteration processes. Models range from progressive alteration within a parent-body environment [1, 3, 4] to the possibility that significant alteration occurred in small precursor planetesimals prior to the formation of the CM asteroid [5]. It is important to determine where and when the alteration took place. It is possible that the timescale of alteration is comparable to the <sup>53</sup>Mn half-life (3.7 Ma).

**Observations:** We studied several CM chondrites of different petrographic subtypes (e.g., CM2.0 LAP 02277, CM2.1 QUE 93005, CM2.2 Cold Bokkeveld, CM2.4/2.5 Murray, CM2.5 Murchison). We used SEM techniques (EDX element maps) as well as electron-probe studies (wavelength-dispersive element maps and quantitative analyses). Element maps show Mn-rich carbonates in QUE 93005 and LAP 02277 as well as Mn-bearing silicates in Murchison. Carbonates are relatively abundant (~2-3 vol.%) and randomly distributed in the thin sections of QUE 93005 and LAP 02277. The carbonates occur as individual crystals as well as irregularly shaped aggregates in QUE 93005 and as single crystals in LAP 02277. We analyzed 25 different carbonate crystals from QUE 93005 by electron-probe. QUE 93005 contains both calcite and/or aragonite (CaCO<sub>3</sub>) and dolomite (CaMg(CO<sub>3</sub>)<sub>2</sub>). Dolomites typically occur as single crystals within larger calcite crystals. Most calcite crystals range between 50 and 100 μm, dolomite grains are typically 10-30 μm. The analyses show enrichments of Mn in several carbonate grains, indicating their suitability for Mn-Cr isotopic studies. MnO contents in calcites range between 0.05 and 0.86 wt.% with an average of 0.19 wt.%. Dolomites are characterized by higher MnO contents, ranging between 1.8 and 4.5 wt.% with an average content of 3.4 wt.%.

**Discussion and future work:** In order to constrain the timing of carbonate formation, we will use the CAMECA ims 1270 ion microprobe at UCLA to study the Mn-Cr systematics of Mn-rich phases in CM chondrites that have undergone different degrees of aqueous alteration. We will focus our study on large carbonate and silicate grains with high Mn/Cr ratios, two important prerequisites for the search for radiogenic <sup>53</sup>Cr formed from the decay of <sup>53</sup>Mn. Published data for CM chondrites show initial <sup>53</sup>Mn/<sup>55</sup>Mn ratios of  $(5.0 \pm 1.5) \times 10^{-6}$  for ALH84034 [6], and  $(1.31 \pm 0.6) \times 10^{-5}$  for Y791198 [7]. Our new data for CM chondrites will help constrain the timescale of aqueous alteration.

**References:** [1] Zolensky M.E. and McSween H.Y. 1988. In *Meteorites and the Early Solar System*. 114-143. [2] Brearley A.J. and Jones R.H. 1998. *Rev. Mineral.* 36: pp. 398. [3] McSween H. Y. 1987. *Geochim. Cosmochim. Acta* 51: 2469-2477. [4] Rubin A.E. et al. 2006. *Geochim. Cosmochim. Acta*, submitted. [5] Bischoff A. 1998. *Meteorit. Planet. Sci.* 33: 1113-1122. [6] Brearley A.J. and Hutcheon I. 2000. Abstract #1407, *Lunar Planet. Sci.* 31. [7] Brearley A.J. and Hutcheon I. 2002. *Meteorit. Planet. Sci.* 37: A23.

### CALCULATIONS OF HEATING CAUSED BY IMPACTS OF POROUS BODIES IN THE EARLY SOLAR SYSTEM

Paul S. De Carli<sup>1</sup> and John Wasson<sup>2</sup>. <sup>1</sup>SRI International, Menlo Park CA 94025 paul.decarli@sri.com, <sup>2</sup>UCLA, Los Angeles CA 90095

**Introduction:** Wasson, Rubin, and others have suggested that shock compression provided a significant source of heating for planetesimals in the early solar system. It seems reasonable to assume that early planetesimals comprised porous aggregates of mm-size grains. Here we present calculations of heating due to impacts between porous bodies.

**Method:** The Autodyn(TM) wave propagation code was used to calculate the impact of a 1-km radius projectile on a 20 km-radius target body. These calculations scale for any projectile mass, provided that the target dimensions are at least an order of magnitude greater than the projectile. Both bodies were modeled as chondritic with volume fractions of .38 pyroxene, .39 olivine, .07 albite, .06 troilite, and .1 Fe-10Ni. Compression and thermal data for the mineral constituents served as the basis for construction of a synthetic Hugoniot for the solid and for construction of a synthetic heat capacity vs. temperature table. We constructed a P-alpha equation of state for a 50 % porous initial material (1.84 g/cc), compressing to the appropriate solid compression curve at 5 GPa. To date, calculations have been carried out for impact velocities of 5 km/s, 7 km/s, and 10 km/s. Pressure histories were recorded at up to 150 stations in the target volume of interest. The peak pressure at each station was equated to the increase in internal energy due to shock compression followed by adiabatic pressure release. We then calculated the mass of target material relative to the projectile mass, Mp, in each of 4 post-shock temperature bins.. Bin 1, 1500-2100K, corresponds to internal energy increases in the range of 1.4-2.3 kJ/g and peak pressures in the range of 10.2 GPa to 16.6 GPa. Bin 2, 2100-2400 K (complete melting), corresponds to internal energy increases in the range of 2.3-3.5 kJ/g and peak pressures in the range of 16.6 GPa-25.4 GPa. Bin 3, 2400->3000K (incipient/partial vaporization), internal energy increase 3.5-5 kJ/g and peak pressures in range of 25.4-36.2 GPa. Bin 4 covers the internal energy range from 5 kJ/g up to about 12 kJ/g, still in the partial vaporization regime > 3000K.

**Results:** Preliminary results show that impact velocities in excess of 5 km/s are required for substantial melt production in the case of impacts between 50% porous bodies of chondritic composition.

Impact velocity	Bin 1, 1500-2100 K	Bin 2, 2100-2400 K	Bin 3, 2400->3000 K	Bin 4, >3000 K, <12 kJ/g
10 km/s	3 Mp	1 Mp	0.98 Mp	1.74 Mp
7 km/s	1.13 Mp	1.3 Mp	0.44 Mp	0.8 Mp
5 km/s	0.66	0.2	0	0

## INDUCTION HEATING IN ASTEROIDS PART 1: OBSERVATIONS AND THEORY

D. N. Della-Giustina, C. A. Marsh, J. Giacalone, and D. S. Lauretta. University of Arizona, Lunar and Planetary Laboratory, Tucson, AZ 87521, USA. Email: dellagiu@email.arizona.edu

**Introduction:** Induction heating, or Joule heating, is the release of thermal energy within a body due to the resistance of that material to a current passing through it. Electromagnetic induction by the T Tauri solar winds has been proposed as a heating mechanism in the early solar system, and could have contributed to the thermal metamorphism and melting in planetesimals [1]. In order for electromagnetic induction to occur a magnetic field of sufficient strength must sweep through a finitely conductive planetesimal inducing a current. Such a magnetic field would originate in the T Tauri sun and propagate through the early solar winds. In recent years the induction heating theory has lost favor as a viable mechanism because the estimated T Tauri solar wind flux along the ecliptic was thought to be too weak to produce significant heating in planetesimals bodies [2].

Recently, the Chandra X-ray observatory completed a 13-day observation in the Orion Cluster of Young Stellar Objects (YSOs) comparable in mass to the early Sun [3]. Twenty-eight of these YSOs, located in the COUP field, emitted intense X-ray flares an average of 1.5 times over a 9 day interval of observation. The average flare luminosity of these objects was calculated to be  $10^{3.8}$  ergs/s [4]. Using the characteristics of the X-ray flares Favata et al. [3] measured the minimum magnetic field necessary to confine the flaring plasma in the stellar corona of these objects. Results yielded a wide range of magnetic field strengths that range between 12 and 3480 Gauss with flare lengths of 0.002 to 0.216 AU. In contrast the magnetic field strength in the modern solar corona is on the order of milliGauss [5]. The data derived from [3] demonstrate that the magnetic structures around these YSOs are in many cases significantly larger than the objects themselves. The presence of such extended magnetic fields suggest that they connect the stellar photosphere with the inner rim of a protoplanetary disk [3].

**Conclusions:** These magnetic field strength measurements indicate that the fields around these objects maintain enough intensity to validate the induction heating model. Although this evidence does not provide the direct magnetic field measurements in the estimated region of planetesimal formation, it does prompt the feasibility of electromagnetic induction to be re-evaluated as a viable heating mechanism in the early solar system [4]. We are reevaluating this theory with a larger magnetic field strength using mathematic modeling and the magnetic field strength around the COUP field YSOs. We determine that field strengths in the region of the modern asteroid belt were on the order of 10-20 Gauss. These values inform the experimental simulation of this process [6].

**References:** [1] Sonett, C.P., *et al.* 1968. *Nature* 219. [2] Wood, J.A., Pellas, P. 1991. *The Sun in Time*. [3] Favata, F., *et al.* 2005. *Astrophysics Journal Supplement Series* 160: 469-502. [4] Marsh, C.A., *et al.* 2006. Abstract # 2078. 37<sup>th</sup> Lunar & Planetary Science Conference. [5] Mancuso, S., Spangler, S. R. 2000. *Astrophysics Journal* 539: 480. [6] Marsh, C.A., *et al.* 2006 69<sup>th</sup> Meteoritical Society (this meeting).

### IDENTIFICATION OF A COMMON R-CHONDRITE IMPACTOR ON THE UREILITE PARENT BODY.

H Downes<sup>1,2</sup> and D W Mittlefehldt<sup>3</sup>. <sup>1</sup>Birkbeck University of London, Malet St. London, WC1E 7HX UK. E-mail: h.downes@ucl.ac.uk; <sup>2</sup>Lunar and Planetary Institute, Houston Texas 77054 USA, <sup>3</sup>Johnson Space Centre, Nasa Rd 1, Houston, Texas USA.

**Introduction:** Polymict ureilites are brecciated ultramafic meteorites that contain a variety of single mineral and lithic clasts [1]. They represent the surface debris from a small, differentiated asteroid. We are continuing a detailed petrological study of several polymict ureilites including EET 87720, EET 83309 and FRO93008 (from Antarctica), North Haig, Nilpena (Australia), DaG 976, DaG 999, DaG 1000 and DaG 1023 (Libya). The latter four stones are probably paired. Clast sizes can be 10 mm in diameter, so a thin-section can consist of a single lithic clast.

**Clast types and compositions:** The most common clast-types are ureilitic olivines and pyroxenes that cover the range of mg# (74-96) and Fe/Mn values observed in monomict ureilites [2]. Among the non-ureilitic mineral clasts are a variety of olivine and pyroxene grains with variable mg#s and distinct minor element contents, some of which may represent as-yet unsampled chondritic bodies. Among the lithic clasts is a type dominated by ferroan olivine (mg# = 59-65), with subordinate sodic plagioclase, orthopyroxene, chromite and pyrrhotite. These clasts have variable recrystallised metamorphic textures, ranging from fine to medium grained and generally lack chondrules. We have found them in EET 87720, EET 83309 and DaG 999/DaG1000. Similar ferroan olivines were previously described in polymict ureilites DaG 319 [3], FRO 93008 [4] and DaG 164 [5] and they likely represent a common impactor on the ureilite parent body.

**R-chondrite origin of impactor clasts:** Clasts in DaG 319 were suggested to be derived from an R-chondrite, but oxygen isotope data on one of these resembled ordinary chondrites [6]. The olivines in these clasts clearly differ from those in the ureilites, not only in their low mg#s but also in their low Cr and Ca and high Ni contents. Their compositions very closely resemble those of olivines in R-chondrites such as Rumuruti [7], Acfer 217 [8], PCA 91002 [9], Carlisle Lakes and ALH 85151 [10]. Furthermore, the presence of chromite and pyrrhotite and the absence of metal also suggest a strong similarity to R-chondrites. Similar R-chondrite lithic clasts have also been reported from Weatherford [11] and Kaidun [12], suggesting that R-chondrite projectiles may have been common impactors on carbonaceous clan asteroids in the early Solar System.

**References:** [1] Goodrich C A et al. 2004. *Chemie der Erde* 64, 283-327. [2] Downes H and Mittlefehldt D W. Abstract #1150 37<sup>th</sup> Lunar & Planetary Science Conference. [3] Ikeda Y et al. 2000. *Antarctic Meteorite Research* 13, 177-221. [4] Fioretti A M and Goodrich C A 2001. 64<sup>th</sup> Annual Meteoritical Society Meeting abstract # 5003. [5] Cohen B, Goodrich C A and Keil K 2004. *GCA* 68, 4249-4266. [6] Ikeda Y et al 2003. *Antarctic Meteorite Research* 16, 105-127. [7] Schulze H et al 1994. *Meteoritics* 29, 275-286. [8] Bischoff A et al 1994. *Meteoritics* 29, 264-274 [9] Rubin A E and Kallemeyn G W 1994. *Meteoritics* 29, 255-264. [10] Rubin A E and Kallemeyn G W 1989. *Geochimica et Cosmochimica Acta* 53, 3035-3044. [11] Prinz et al. 1993. *Meteoritics* 28, 419. [12] Zolensky M and Ivanov A 2003. *Chemie Der Erde* 63, 185-246.

### ORIGIN OF THE HALOGENS IN THE DARK MATRIX OF RUMURUTI.

G. Dreibus, W. Huisl, B. Spettel, and R. Haubold, Max-Planck-Institut f. Chemie, P.O. BOX 3060, D-55020 Mainz, Germany; dreibus@mpch-mainz.mpg.de

**Introduction:** Rumuruti is a regolith breccia with typical light – dark structure and has solar-wind-implanted gases [1, 2]. The first analyses with INAA of two whole rock samples from a large light-colored clast (110 mg) and from the dark matrix (90 mg) gave identical compositions of both lithologies, except for the enrichment of C, Br, and Hg in the dark matrix. The other halogens could not be measured [1]. In a new aliquot of the dark matrix all halogens were measured by RNAA and an ionselective electrode and compared with the gas-rich H5-chondrite regolith breccia Pantar.

**Results:** Measured halogens and other volatile and moderately volatile elements are as follows:

	Rum.	Rum.	Rum.	CM	H3	H5	H5
*	1	2	3	4	5	6	7
wt. [mg]	90	113	110	207	129	102	101
S [%]	4.14		3.99	3.07	2.2		
F [ppm]		<30		38	13	8	8
Cl		282		180	303	119	75
Br	1.2	1.19	0.41	0.75	1.15	0.79	0.25
J		0.22		0.19		0.21	0.03
C	740		420	17100			
Se	14.4	14	14.7	12.9	7.9	8.5	9.3
Zn	165	157	160	180	44	54	50
Na	6900	6790	6780	1740	6760	5900	5700
K	693	816	820	310	505	790	
Mn	2270	2230	2270	1560	2420	2300	2300

\*1: Rumuruti, dark matrix [1]; 2: Rumuruti, dark matrix, this work; 3: Rumuruti, light clast [1]; 4: Murchison, this work; 5: Tieschitz, this work and [3]; 6: Pantar dark, this work and [4]; 7: Pantar light, this work and [4].

The concentrations of Cl, Br, and J in the dark matrix of Rumuruti are similar to carbonaceous chondrites (CM), Tieschitz (H3) and the dark matrix of Pantar. The abundances of the moderately volatiles S, Se and Zn are similar to CM and show no variations between dark and light matrix in Rumuruti as also found in ordinary chondrites (see table). Br is enriched in the dark matrix relative to the light clast by a factor of 3 which we also found for both components in the gas-rich regolith breccia Pantar. The heterogeneous distribution of the highly volatile halogens in the gasrich regolith breccias Rumuruti and ordinary chondrites could be caused by redistribution processes during thermal metamorphism or by interaction with fluid phases on their parent bodies.

**References:** [1] Schulze H. et al. 1997. *Meteoritics* 29:275-286. [2] Weber H. W. and Schultz L. 1995. *Meteoritics* 30:A596. [3] Kallemeyn G. W. et al. 1989. *Geochimica et Cosmochimica Acta* 53:2747-2781. [4] Lipschutz M. E. et al. 1983. *Geochimica et Cosmochimica Acta* 47:169-181.

**IS MARTIAN SURFACE TYPE 1 MILDLY ALKALINE?:  
RESULTS FROM NEW LINEAR DECONVOLUTIONS OF  
SURFACE TYPES 1 AND 2.**

T.L. Dunn<sup>1</sup> and H.Y. McSween, Jr.<sup>1</sup> Department of Earth and Planetary Sciences, University of Tennessee, Knoxville, TN 37996. tdunn@utk.edu.

**Introduction:** The Thermal Emission Spectrometer (TES) uses thermal infrared energy emitted from the Martian surface to identify rock compositions and surface lithologies [1]. TES analyses have identified two compositionally distinct surface types on Mars [2,3]. Surface type 1 is basalt, and surface type 2 has been suggested to be either andesite [2,3] or partially weathered basalt [4,5]. Both of these volcanic surface compositions are subalkaline, but evidence from Gusev Crater rocks analyzed by the Spirit Rover suggests alkalic magmatism may also have occurred on Mars [6]. This assertion is also supported by evidence from SNC meteorites. For example, mineral assemblages and LREE enriched signatures of the Chassigny meteorite are comparable to those of some terrestrial alkalic magmas, prompting [7] to propose that Chassigny may have formed from an alkalic magma. Also, fractional crystallization modeling [8] of a parental magma composition for Nakhla produces an alkaline liquid line of descent [9]. These observations suggest that Martian volcanism may not have been strictly subalkaline, as current remote sensing data would suggest.

**Methodology:** To test the validity of the assessment of surface type 1 and 2 as subalkaline rocks, ST1 and ST2 were linearly deconvolved [10] using an end-member suite tailored for mildly alkaline volcanic rocks. Modal mineralogies were determined directly from the linear deconvolution algorithm, and bulk rock chemistries were derived from modeled mineralogies by combining endmember compositions in proportion to their abundances and recalculating to wt%. Our modeled modal mineralogies and derived bulk rock chemistries were then compared to previous deconvolutions of surface types 1 and 2 [2,3,4].

**Results:** Deconvolution of surface types 1 and 2 spectra using an end-member set tailored for alkalic rocks produces modal mineralogies that are distinct from previous deconvolutions using subalkaline end-member sets [2,3,4]. Derived chemical compositions of surface type 2 are similar to previous estimates, confirming that surface type 2 is subalkaline. Surface type 1, however, is more alkaline than previous results. Using [11], surface type 1 is classified as a basaltic trachyandesite rather than a basalt. Combined with evidence from Gusev Crater rocks and SNC meteorites, this may suggest that some surface type 1 regions could contain alkalic rocks. The average surface type 1 spectrum, however, is not definitive.

**References:** [1] Christensen P.R. et al. (2000) *JGR*, 106, 23,823-23,871. [2] Bandfield J.L. et al. (2000) *Science*, 287, 1626-1630. [3] Hamilton V.E. et al. (2001) *JGR* 106, 14,733-14,746. [4] Wyatt M.B. and McSween H.Y. (2002) *Nature*, 417, 263-266. [5] Michalski J.R. et al. (2005) *Icarus* 174, 161-177. [6] McSween H.Y. et al. (2006) *LPSC XXXVII*, Abstract # 1120 [7] Nekvasil H. (2003) 6<sup>th</sup> *Mars Conf.*, Abstract # 3041 [8] Ghorso M.S. and Sack R.O. (1995) *Contr. Min. Pet.* 119, 197-212. [9] Stockstill K.R. et al. (2005) *Meteor. Plan. Sci.*, 40, 377-396. [10] Ramsey M.S. and Christensen P.R. (1998) *JGR*, 103, 577-596. [11] Le Bas M.J. et al. (1986) *J. Pet.*, 27, 745-750.

**THE MICROMETEORITE MASS FLUX AS RECORDED IN DOME C CENTRAL ANTARCTIC SURFACE SNOW.**

J. Duprat<sup>1</sup>, C. Engrand<sup>1</sup>, M. Maurette<sup>1</sup>, F. Naulin<sup>1</sup>, G. Kurat<sup>2</sup>, M. Gounelle<sup>3</sup>, <sup>1</sup>CSNSM, Bat.104, 91405 Orsay, Fr., <sup>2</sup>Univ. Wien, Inst. Geol. Wissenschaft, A-1090 Vienna, Austria. <sup>3</sup>MNHN, 57 rue Cuvier, 75231 Paris, Fr.

**Introduction:** We used the unique characteristics of central Antarctic surface snow to revisit the issue of the extraterrestrial (ET) dust flux reaching the Earth's surface. Marine osmium isotopic data indicate an average flux of ET material of  $30 \times 10^3$  tons/yr [1], in agreement with flux of micrometeoroids before atmospheric entry [2]. On short time scales (< Myrs), the bulk of ET material comes from dust with sizes  $\sim 200$   $\mu$ m [2]. Still a challenging issue is to estimate the fraction of this flux that actually reaches the Earth surface as particles (i.e. micrometeorites) from the one that it vaporized during atmospheric entry.

**Experimental procedure and results:** The evaluation of the micrometeorite (MM) flux requires an accurate control on several critical parameters: i) the equivalent exposition surface, S, (in  $\text{m}^2 \cdot \text{yr}$ ), ii) the collection efficiency, iii) the potential statistical biases. In January 2002, we collected MMs at CONCORDIA station at Dome C ( $75^\circ\text{S}$ - $123^\circ\text{E}$ ). A total of  $10 \text{ m}^3$  of snow were manually extracted in a clean trench at 4 m depth, corresponding to  $S \sim 100 \text{ m}^2 \cdot \text{yr}$ . This snow was melted and sieved down to  $30 \mu\text{m}$  in a dedicated ultra-clean stainless steel snow smelter allowing us to measure, for each melt, the collection efficiency in two size ranges ( $30$ - $100 \mu\text{m}$  and  $>100 \mu\text{m}$ ). Dome C snow is well protected from terrestrial dust within the  $>30 \mu\text{m}$  size range allowing the analysis of all the particles contained in the filters. The collection technique used and the unique conditions of Dome C snow allow recovering of all types of ET particles, i.e. both melted and unmelted. We identified by SEM imaging and EDX analysis a total of 500 MMs. The accumulation rate at Dome C is low and regular [3], thus the S parameter can be deduced accurately for each melt. The 10 consecutive melts yielded 10 independent flux values ranging from  $3 \times 10^3$  up to  $10 \times 10^3$  tons/yr. The large variations of these values can be understood as resulting from statistical sampling. Following [1], we developed a Monte Carlo numerical code simulating the expected flux. We find an average MM flux at Dome C of 5300 tons/yr. The flux of MMs at Earth surface represent no more than 1/3 of the total incoming flux of particles before atmospheric entry, in agreement with recent studies conducted in Antarctic snow [4] and ice [5]. We will discuss the various sources of uncertainties for all these different studies and emphasize the assets of the present work as well as the corrections that have to be applied to both CONCORDIA flux and to values determined before atmospheric entry [1,6]. Finally, we will present the high statistics MMs collection we performed at CONCORDIA in January 2006.

**Acknowledgements:** We thank IPEV and PNRA for funding and logistical support to the CONCORDIA micrometeorite collection at Dome C.

**References:** [1] B. Peucker-Ehrenbrink and G. Ravizza, *GCA*, 2000. **64**(11): p. 1965-1970. [2] S. G. Love and D. E. Brownlee, *Science*, 1993. **262**: p. 550-553. [3] J.-R. Petit, et al., *JRS*, 1982. **87**: p. 4301-4308. [4] S. Taylor, et al., *Science*, 1998. **392**: p. 899-903. [5] T. Yada, et al., *EPSL*, 2004. **56**: p. 67-79. [6] E. Grün, et al., 2001. *Interplanetary dust*: Berlin, Springer.